Networks and Heterogeneous Media

https://www.aimspress.com/journal/nhm

NHM, 21(7): 2526–2555.
DOI: 10.3934/nhm.2026094
Received: 27 August 2026
Revised: 16 November 2026
Accepted: 23 November 2026
Published: 27 November 2026

Research article

Dynamics of a fractional-order SWFPR rumor propagation model with a fear effect and delayed official refutation

Jiaqi Wang and Ahmadjan Muhammadhaji*

College of Mathematics and Systems Science, Xinjiang University, Urumqi 830017, China

* **Correspondence:** Email: ahmatjanam@aliyun.com.

Abstract: Online rumors spread rapidly and severely threaten public opinion, and timely official refutation is an effective way to suppress rumor diffusion. This work established a fractional-order delayed Susceptible–Waverer–Fearful–Propagator–Recovered (SWFPR) compartmental rumor propagation model incorporating a fear effect and dual debunking mechanisms under the Caputo fractional derivative framework. The fractional order describes the memory effect of historical rumor information on individual behavior. We first proved the positivity, existence, uniqueness, and ultimate boundedness of model solutions. Then we analyzed the existence of equilibrium points and derived the stability conditions of rumor-free and rumor-endemic equilibria. By selecting the time delay as the bifurcation parameter, we investigated the Hopf bifurcation of the system and discussed the dynamical influence of the fear effect and refutation delay on rumor prevalence. Numerical simulations were carried out to verify the theoretical results and illustrate the impacts of fractional order, fear intensity, and refutation delay on rumor evolution. The results revealed that an excessively long refutation delay facilitates rumor outbreaks, while the fear effect can inhibit the persistent prevalence of rumors. This work provides theoretical support for understanding rumor dynamics and designing targeted rumor intervention strategies on social media.

Keywords: rumor propagation model; fear effect; fractional order; time delay; Hopf bifurcation

1. Introduction

In the information age, fueled by ongoing digital transformation, online social-networking platforms have become the primary channel for information spread, whereas rumors have grown into a typical form of distorted information marked by sudden occurrence, intense emotional inclination, and fission-style fast propagation. Such unfounded and deceptive content has an irreversible and far-reaching negative impact on regular social operations, daily public safety, and long-term national stability. Concrete cases ranging from goods hoarding and social panic sparked by epidemic-related

false information, public opinion disorder, and biased spreading caused by unexpected public incidents to online reputation infringement and rights abuse driven by fabricated rumors have indicated the pressing necessity for both academic researchers and practical management departments to thoroughly explore the intricate mechanisms of rumor spread and develop scientific and targeted dynamic forecasting models.

Rumor diffusion shares substantial and inherent similarities with the transmission of infectious diseases and offers a mature and feasible interdisciplinary research approach for the quantitative analysis of rumor dynamics. Concretely, both types of spreading processes abide by the core compartmental pattern of "susceptible spreader/infected immune" dividing the target population into distinct states based on information acceptance or disease infection status; both realize continuous transmission via frequent interpersonal contacts and interactions, and their spreading trends are co-determined by core transmission parameters, recovery transition rates, and social-network structure. Additionally, both possess a vital propagation threshold that determines whether diffusion can maintain its long-term existence and show clearly staged dynamic features from the initial outbreak to gradual fade-out. Accordingly, their prevention and control approaches are highly similar: blocking effective transmission routes to halt continuous spread, enhancing overall group immunity (referring to official rumor refutation and vaccine inoculation, in turn), and focusing on high-risk groups to reduce the strength and range of diffusion.

In 1964, Daley and Kendall [1] established a crucial interdisciplinary connection between infectious disease dynamics and rumor propagation by proposing an Susceptible–Infected–Recovered (SIR)-based rumor model, laying the initial theoretical groundwork for the systematic development of rumor dynamic modeling. They further optimized the model framework and developed the first discrete stochastic Daley–Kendall (DK) model in 1965, which accurately portrayed the entire dynamic evolution of rumors from generation to gradual extinction [2]. In 1973, Maki and Thompson [3] investigated the inherent drawbacks of the early DK model in describing individual spreading behaviors, adjusted the model structure, and proposed the classical Maki–Thompson (MK) model, which became a vital cornerstone for subsequent research. Since then, numerous scholars have continuously extended and revised these classical model frameworks, driving the steady advancement of rumor-modeling theory and its practical applications [4–8]. Nevertheless, conventional integer-order dynamic models cannot fully reflect the complexity of real rumor propagation, particularly nonlinear diffusion trajectories and the long-term memory effects of historical information states. In contrast, fractional-order models have distinctive merits in depicting a system's historical dependence and complex nonlinear dynamics with tunable order parameters, making them more suitable for matching the irregular and variable laws of actual rumor spread [9]. For example, De Santis et al. [10] proposed a fractional-order Susceptible–Infected–Vaccinated–Recovered (SIVR) model aimed at spreading fake news on social platforms, and Niu et al. [11] established a time-delayed fractional-order Ignorant–Discussant–Spreader–Remover (IDSR) model that considers dynamic lag features in rumor transmission.

The fear effect serves as a key psychological catalyst throughout the process of rumor propagation, triggering the dual individual psychological motives of self-protection and altruistic reminders to surrounding people, impairing the ability of rational information identification and independent decision-making, and further inducing large-scale group emotional contagion. This series of psychological and behavioral shifts directly boosts the spreading speed, coverage range, and duration

of rumors, and even leads to mass panic and social chaos in extreme cases [12]. In the preliminary theoretical study of rumor psychology, Knapp [13] systematically demonstrated the core driving role of fear in the emergence and spread of rumors from a theoretical perspective, clarifying the close internal link between negative emotional factors and rumor diffusion. Subsequently, Pfattheicher et al. [14] and Stieglitz et al. [15] conducted targeted empirical investigations in practical scenarios, such as public health emergencies and sudden natural disasters, providing solid and reliable empirical proof for the facilitating effect of fear on rumor spread, and further confirmed the necessity of incorporating fear factors into rumor dynamic models.

Official rumor refutation is universally recognized as the core and most efficient means of curbing the sustained spread of rumors, rectifying public cognitive deviations, and stabilizing social public opinion. However, various time-delay factors significantly increase the complexity of rumor dynamic modeling. These time lags mainly consist of the natural fermentation stage of rumors, the verification delay in official information collection and fact-checking, and the public's cognitive lag in accepting and trusting refutation content. However, current studies rarely dissect the detailed dynamic mechanisms of these time delays in rumor propagation, and most existing models fail to effectively interpret typical phenomena, including rumor rebound and long-term persistence [16–18]. Hence, this study elaborates on the complete mechanism of official rumor refutation, quantifies the regulatory impact of time delays on the entire propagation process, and builds an improved fractional-order time-delayed rumor propagation model integrating the fear compartment (F) and official refutation rate, namely, the SWFPR model, with the purpose of filling current research gaps and offering targeted theoretical support for the prevention and governance of public opinion crises.

Compared with existing rumor-propagation dynamic models, the present study possesses several distinct improvements. First, traditional rumor models mainly employ SIR-like low-dimensional compartment frameworks, which cannot well-separate users with indecisive mental status and users suffering rumor-triggered fear. This paper constructs a five-compartment SWFPR model by introducing the waverer compartment W and fearful compartment F, which distinguishes individuals who merely access rumor content from those who form negative fear psychology. Second, in most existing epidemic-like rumor models involving fear effects, fear is implemented as a static coefficient modifying transmission rates. Differing from those treatments, fear in our system is modeled as an independent state variable $F(t)$. Population flows into the fearful compartment via rumor contact, and fearful individuals further turn into active rumor propagators, which reproduces the gradual accumulation of negative sentiment in real social scenarios. Third, although prior literature has considered various kinds of time delays in rumor dynamics, few works focus on the time lag between fear generation and subsequent rumor-spreading actions. In our fractional-order delayed model, τ represents the emotional accumulation delay: there exists a time gap after individuals develop fear before they start to propagate rumors. This mechanism provides a potential dynamical interpretation for real-world phenomena such as rumor recurrence and long-term persistence.

The rest of this paper is organized as follows. Section 2 reviews the fundamental theories of fractional-order dynamics and classical rumor propagation models. Section 3 elaborates on the proposed fractional-order time-delayed SWFPR model, including model assumptions, parameter definitions, and the formulation of dynamic equations. Section 4 investigates the positivity, existence, uniqueness, and ultimate boundedness of solutions, equilibrium stability, and Hopf bifurcation characteristics of the established model. Section 5 performs comprehensive numerical simulations to

verify the theoretical results and examine the effects of key parameters. Section 6 summarizes the main findings of this study and discusses potential directions for future work.

2. Preliminaries

This paper adopts the following definitions and lemmas as the theoretical foundation for the subsequent proofs.

Definition 2.1. *The Caputo-type fractional-order derivative is defined as [11]:*

$$ {}_{t_0}^{C}D_t^{\theta} f(t) = \frac{1}{\Gamma(n-\theta)} \int_{t_0}^{t} \frac{f^{(n)}(\tau)}{(t-\tau)^{\theta+1-n}} \mathrm{d}\tau, $$

where n is a positive integer, θ denotes the order of the fractional derivative with $n-1 < \theta < n$, $\Gamma(\cdot)$ represents the gamma function, and its expression is given by:

$$ \Gamma(h) = \int_0^{\infty} t^{h-1} e^{-t} \mathrm{d}t, \quad \mathrm{Re}(h) > 0. $$

For social-media rumor spreading, the memory property encoded in the Caputo fractional-order derivative describes the cumulative influence of historical information and lingering public psychological impressions left by past rumor events. The fractional order $\theta \in (0, 1]$ quantifies the strength of this memory effect: (i) A smaller θ yields stronger long-term memory. User behaviors and state transitions are persistently shaped by earlier rumor-related content; impressions of historical public-opinion events decay slowly. (ii) As θ approaches 1, the Caputo derivative reduces to the standard integer-order derivative. The memory effect becomes negligible, and individual behavioral choices are dominated by instant, real-time information. Recent advances in fractional-order compartmental modeling have demonstrated the capacity of fractional derivatives to characterize memory-dependent spreading dynamics for epidemic and misinformation processes, with theoretical analysis and practical applications reported in [19, 20].

Remark 1. It is worth noting that another widely used operator, the Riemann–Liouville fractional derivative, involves fractional-order initial values which have no straightforward psychological interpretation for human populations. By contrast, the Caputo derivative adopts integer-order initial conditions consistent with real-world social survey data, making it more appropriate for modeling human-driven rumor-spreading systems.

Lemma 2.1. *If all the eigenvalues of matrix Q have negative real parts, then it can be concluded that the zero solution of system*

$$ {}_{0}^{C}D_t^{\theta} \boldsymbol{Z}(t) = \boldsymbol{Q}\boldsymbol{Z}, \quad \theta \in (0, 1), \quad \boldsymbol{Q} \in \mathbf{R}^{n\times n}, \ \boldsymbol{Z} \in \mathbf{R}^{n}, $$

is asymptotically stable [21].

Lemma 2.2. *Let $f(t)$ be a continuous function satisfying the exponential order condition. Specifically, there exist positive constants M and σ such that $|f(t)| \le Me^{\sigma t}$ holds for all $t \ge 0$. Let ${}_{0}^{C}D_t^{\theta} f(t)$ denote the Caputo fractional derivative of $f(t)$, where the fractional order θ satisfies $n-1 < \theta < n$ (n is a positive integer, i.e., $n \in \mathbb{N}$).*

The Laplace transform of the Caputo fractional derivative ${}_0^C D_t^\theta f(t)$ is given by the following formula [22]:

$$\mathcal{L}\left\{{}_0^C D_t^\theta f(t)\right\}(s) = s^\theta F(s) - \sum_{k=0}^{n-1} s^{k-n+\theta} f^{(k)}(0^+),$$

where:

- $\mathcal{L}\{f(t)\}(s) = F(s)$*: the Laplace transform of the function* $f(t)$*;*
- $f^{(k)}(0^+)$*: the k-th right-hand derivative of* $f(t)$ *at the point* $t = 0$*;*
- $\mathcal{L}\{\cdot\}$*: the Laplace transform operator.*

Lemma 2.3. *Consider the following n-dimensional linear fractional-order system with multiple time delays [11]:*

$$\begin{cases} {}_0^C D_t^{\theta_1} y_1(t) = z_{11} y_1(t-\tau_{11}) + z_{12} y_2(t-\tau_{12}) + \cdots + z_{1n} y_n(t-\tau_{1n}), \\ {}_0^C D_t^{\theta_2} y_2(t) = z_{21} y_1(t-\tau_{21}) + z_{22} y_2(t-\tau_{22}) + \cdots + z_{2n} y_n(t-\tau_{2n}), \\ \qquad\qquad \vdots \\ {}_0^C D_t^{\theta_n} y_n(t) = z_{n1} y_1(t-\tau_{n1}) + z_{n2} y_2(t-\tau_{n2}) + \cdots + z_{nn} y_n(t-\tau_{nn}), \end{cases} \tag{2.1}$$

where $\theta_i \in (0,1)$ *is the fractional order,* $\tau_{ij} > 0$ *is the time delay,* $y(t) = (y_1(t), y_2(t), \cdots, y_n(t))$ *is the state vector,* $y_i(t) = \Phi_i(t), -\tau_{\max} \le t \le 0$ $(i, j = 1, 2, \cdots, n)$ *represents the initial condition,* $\tau_{\max} = \max\{\tau_{ij} \mid i, j = 1, 2, \cdots, n\}$*, and* $Q = [z_{ij}]_{n\times n} \in \mathbb{R}^{n\times n}$ *is the coefficient matrix. The characteristic matrix of the system is written as*

$$\triangle(s) = \begin{pmatrix} s^{\theta_1} - z_{11}e^{-s\tau_{11}} & -z_{12}e^{-s\tau_{12}} & \cdots & -z_{1n}e^{-s\tau_{1n}} \\ -z_{21}e^{-s\tau_{21}} & s^{\theta_2} - z_{22}e^{-s\tau_{22}} & \cdots & -z_{2n}e^{-s\tau_{2n}} \\ \vdots & \vdots & \ddots & \vdots \\ -z_{n1}e^{-s\tau_{n1}} & -z_{n2}e^{-s\tau_{n2}} & \cdots & s^{\theta_n} - z_{nn}e^{-s\tau_{nn}} \end{pmatrix}.$$

3. Description of the rumor propagation model

Both the spread of infectious diseases and the propagation of rumors exhibit typical dynamic characteristics of population diffusion and state evolution, and they share strong similarities in transmission mechanisms such as contact-driven diffusion and demographic state transitions.

Motivated by this relationship, Mandal et al. [23] developed a family of fractional-order Susceptible–Infected–Susceptible (SIS) epidemic models:

$$\begin{cases} {}_{t_0}^C D_t^\alpha S(t) = \frac{rS}{1+\beta I} - aS - bS^2 - \frac{\gamma S I}{1+\delta I} + (m+u)I, \\ {}_{t_0}^C D_t^\alpha I(t) = \frac{\gamma S I}{1+\delta I} - (m+u)I - (a+d)I, \end{cases} \tag{3.1}$$

which characterize the memory and nonlocality of the transmission process through fractional-order operators. Compared with integer-order models, this type of model is more consistent with the dynamic characteristics of actual transmission systems. Considering that traditional integer-order rumor propagation models find it difficult to accurately describe the lag effect and cumulative impact in rumor spread, this study draws on the modeling framework of the aforementioned fractional-order

epidemic model. Combined with the unique attributes of rumor propagation (such as the fear effect, time delay of cognitive transformation, and impact of official rumor refutation), we extend and generalize the classical integer-order rumor model.

To more accurately characterize the complex dynamical behaviors involved in rumor propagation, a fractional-order model tailored for rumor propagation scenarios is constructed [24]. The proposed model (SWFPR) is presented as follows:

$$\begin{cases} {}_0^C D_t^\theta S(t) = \Pi f(P) S(t) - \alpha_1 S(t) P(t) - a S(t)^2 - \mu S(t) - d S(t), \\ {}_0^C D_t^\theta W(t) = \mu S(t) - \alpha_2 W(t) P(t) - \beta W(t) - d W(t), \\ {}_0^C D_t^\theta F(t) = \alpha_1 S(t) P(t) + \alpha_2 W(t) P(t) - \gamma F(t-\tau) - d F(t), \\ {}_0^C D_t^\theta P(t) = \gamma F(t-\tau) - \eta P(t) - d P(t), \\ {}_0^C D_t^\theta R(t) = \eta P(t) + \beta W(t) - d R(t). \end{cases} \tag{3.2}$$

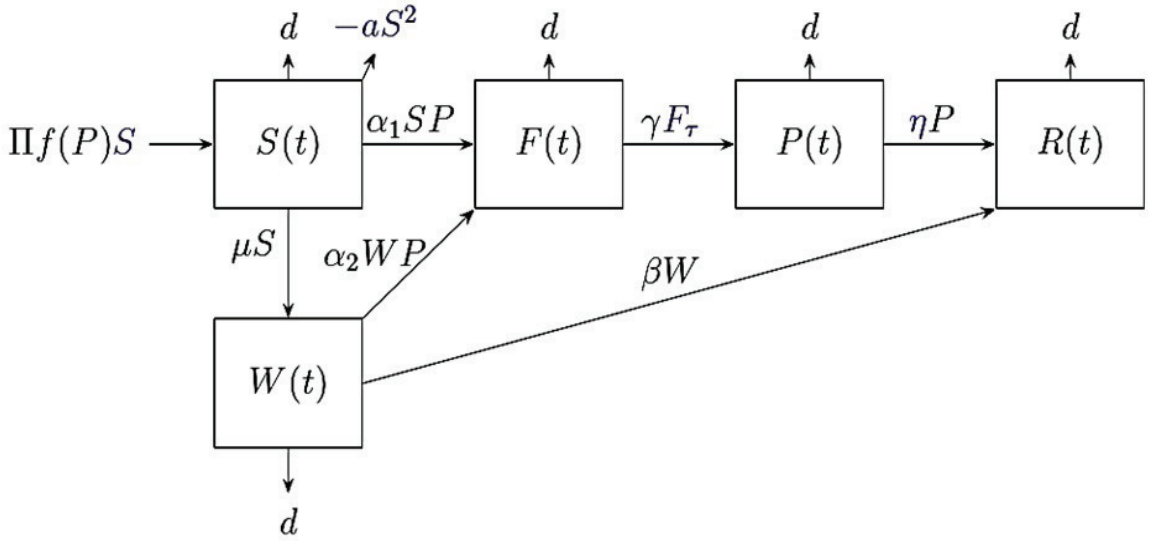

Figure 1. Flow diagram of the SWFPR fractional-order delayed rumor propagation model. Arrows between compartments represent inter-compartment transition fluxes. The outward flux aS^2 from the susceptible compartment S denotes density-dependent attention competition and spontaneous exit of susceptible users. The delayed flux γF_τ describes the transformation from F to P with time delay τ. The transition from P to R follows the flux ηP.

Figure 1 illustrates the state transition mechanism of model (3.2). For this fractional-order rumor propagation system, the meaning of each state variable is specified as follows: $S(t)$, $W(t)$, $F(t)$, $P(t)$, and $R(t)$ denote the densities of susceptible individuals, waverers, fearful individuals, rumor propagators, and recovered individuals at time t, respectively, covering all subgroups with distinct rumor-related contact behaviors. Π describes the baseline activation efficiency of dormant registered users inside social networks, rather than the access frequency of completely new external registrants. The term $\Pi f(P)S(t)$ characterizes the process that dormant users are awakened and converted into susceptible individuals S, and the magnitude of newly activated susceptible individuals is proportional to the existing susceptible population $S(t)$. Symbol d reflects the natural elimination

ratio of all categories, measuring the possibility of active users autonomously quitting the network platforms. μ expresses the conversion ratio of susceptible members to hesitant groups, which measures the likelihood of individuals falling into indecision after touching rumorous information.

Two distinct transmission coefficients, α_1 and α_2, are set separately. α_1 calculates the possibility of conversion from susceptible groups to emotionally fearful groups under rumor diffusion, whereas α_2 quantifies a similar transformation of hesitant individuals under the same spreading impact. γ controls the conversion ratio of fearful crowds to active disseminators, revealing the behavioral tendency driven by negative sentiment to participate in rumor spreading. η describes the self-recovery capacity of the disseminators, indicating the natural fading probability of rumor memories without external intervention. β reflects the comprehensive capacity for official rumor clarification by measuring the conversion proportion toward immune groups after accepting the authoritative correction content. The average degree of connection between social nodes describes the daily information interaction frequency among users, which is an essential topological attribute of the network structure. We adopt a nonlinear influence function $f(P) = \frac{1}{1+\vartheta P}$ to depict the saturation restriction in rumor diffusion, where ϑ serves as the intensity coefficient of negative sentiment and evaluates its suppression effect on spreading actions. The time delay τ describes the lag period of emotional accumulation, referring to the time gap between rumor contact, emotional change, and actual spreading behavior, and effectively reflects the asynchronous feature between individual cognition and practical behavior. The quadratic term $-aS^2$ represents density-dependent attention competition among susceptible users. The per-capita rate at which susceptible individuals lose interest and leave the discussion is proportional to the size of the susceptible population S, giving the total outflow aS^2. This is a spontaneous exit process from the susceptible compartment and is distinct from transmission saturation, which controls the rate of rumor transmission between spreaders and susceptibles. In addition, $f(P)$ acts as an independent global feedback on new-user recruitment modulated by rumor pressure P, so these three mechanisms are decoupled in our model. Here, $\theta \in (0, 1]$, and the model is subject to the following initial conditions:

$$S(\nu) = \phi_1(\nu),\ W(\nu) = \phi_2(\nu),\ F(\nu) = \phi_3(\nu),\ P(\nu) = \phi_4(\nu),$$

$$R(\nu) = \phi_5(\nu),\ \phi_i(\nu) \geq 0,\ \nu \in [-\tau, 0].$$

When the fractional order θ is set to 1, system (3.2) degenerates into a corresponding integer-order rumor propagation model. For the established five-dimensional fractional-order SWFPR model, the recovery variable $R(t)$ is decoupled from the core propagation-related variables $S(t)$, $W(t)$, $F(t)$, and $P(t)$. Specifically, the variation in $R(t)$ only depends on the states of $W(t)$ and $P(t)$, and imposes no reverse influence on the dynamic evolution of the other core variables.

Accordingly, the dynamic analysis of the original five-dimensional system can be simplified to an investigation of a four-dimensional subsystem. To simplify the parametric structure of the model, we ignore the difference between the two transmission rates and impose the equivalent condition $\alpha_2 = \alpha_1$.

4. Main results

In this section, first we investigate the existence, positivity, and uniform boundedness of solutions to system (3.2), and then investigate the stability properties of system (3.2) at its two distinct equilibrium

points. Meanwhile, the Hopf bifurcation dynamics of system (3.2) at E^* are analyzed by taking τ as the bifurcation parameter, and the corresponding critical bifurcation value is determined systematically.

Given the fact that the variable $R(t)$ emerges solely within the terminal equation of system (3.2), the subsequent theoretical analysis concentrates on the reduced subsystem extracted from the fractional-order SWFPR system.

4.1. Existence, uniqueness, positivity, and ultimate boundedness

We consider the Caputo fractional delayed SWFPR rumor propagation system with initial conditions given in Section 3.

Theorem 4.1. (Existence and uniqueness) The fractional-order delayed SWFPR system (3.2) with the given initial conditions admits a unique continuous solution $(S(t), W(t), F(t), P(t), R(t))$ for all $t \geq 0$.

Proof. Define the state-history vector

$$x_t(\nu) = (S(t+\nu), W(t+\nu), F(t+\nu), P(t+\nu), R(t+\nu)), \quad \nu \in [-\tau, 0],$$

and define the vector field generated by system (3.2) as

$$\mathcal{F}(t, x_t) = \begin{pmatrix} \Pi \dfrac{S(t)}{1+\vartheta P(t)} - \alpha_1 S(t)P(t) - aS(t)^2 - (\mu+d)S(t) \\ \mu S(t) - \alpha_2 W(t)P(t) - (\beta+d)W(t) \\ \alpha_1 S(t)P(t) + \alpha_2 W(t)P(t) - \gamma F(t-\tau) - dF(t) \\ \gamma F(t-\tau) - (\eta+d)P(t) \\ \eta P(t) + \beta W(t) - dR(t) \end{pmatrix}.$$

Then, system (3.2) can be written as

$${}_0^C D_t^\theta x(t) = \mathcal{F}(t, x_t), \quad t \geq 0,$$

with the prescribed initial history on $[-\tau, 0]$.

First, $\mathcal{F}(t, x_t)$ is continuous with respect to t and x_t, since all terms are linear, quadratic, or rational functions of the state variables and the delayed state $F(t-\tau)$, and $f(P) = 1/(1+\vartheta P)$ is continuous on any bounded interval not containing $P = -1/\vartheta$.

Next, we verify the local Lipschitz property. Let $\Omega \subset C([-\tau, 0], \mathbb{R}^5)$ be any bounded closed set, and let

$$M_\Omega = \sup_{\phi \in \Omega} \|\phi\|_\infty < +\infty.$$

On the interval $[-M_\Omega, M_\Omega]$, the function $f(P) = 1/(1+\vartheta P)$ is C^1, so there exists $L_f > 0$ such that

$$|f(P_1) - f(P_2)| \leq L_f |P_1 - P_2|.$$

For the bilinear terms, e.g.,

$$|S_1 P_1 - S_2 P_2| \leq |S_1||P_1 - P_2| + |P_2||S_1 - S_2| \leq M_\Omega(|S_1 - S_2| + |P_1 - P_2|),$$

and similarly for WP. The quadratic term satisfies

$$|S_1^2 - S_2^2| \leq 2M_\Omega |S_1 - S_2|.$$

All remaining terms are linear. Therefore, there exists $L_\Omega > 0$ such that

$$\|\mathcal{F}(t, x_t) - \mathcal{F}(t, y_t)\|_{\mathbb{R}^5} \le L_\Omega \|x_t - y_t\|_{C([-\tau,0],\mathbb{R}^5)}.$$

By the standard existence–uniqueness theorem for Caputo fractional delay differential equations [25], system (3.2) has a unique local solution on $[-\tau, T_{\max})$ for some $T_{\max} > 0$.

It remains to justify that $T_{\max} = +\infty$. Suppose, on the contrary, that $T_{\max} < +\infty$. By the non-negativity of solutions (which follows from the same barrier argument as in Theorem 4.2), we have $S(t), W(t), F(t), P(t), R(t) \ge 0$ on $[-\tau, T_{\max})$. Let

$$N(t) = S(t) + W(t) + F(t) + P(t) + R(t).$$

Summing the five equations of system (3.2), all transition terms cancel, and we obtain

$${}_0^C D_t^\theta N(t) = \Pi f(P) S - a S^2 - dN.$$

Since $P(t) \ge 0$, we have $0 \le f(P) = 1/(1 + \vartheta P) \le 1$. Hence

$${}_0^C D_t^\theta N(t) \le \Pi S - a S^2 - dN \le \frac{\Pi^2}{4a} - dN,$$

where $a > 0$. By the comparison principle for Caputo fractional differential equations,

$$N(t) \le N(0) E_\theta(-d t^\theta) + \frac{\Pi^2}{4ad}(1 - E_\theta(-d t^\theta)),$$

where $E_\theta(\cdot)$ is the Mittag–Leffler function. Thus $N(t)$ is bounded on $[0, T_{\max})$ and, consequently, all components S, W, F, P, R are bounded on $[0, T_{\max})$. Therefore, $\mathcal{F}(t, x_t)$ is uniformly bounded on $[0, T_{\max})$; say,

$$\|\mathcal{F}(t, x_t)\| \le C, \quad 0 \le t < T_{\max}.$$

Using the equivalent Volterra integral equation

$$x(t) = x(0) + \frac{1}{\Gamma(\theta)} \int_0^t (t - s)^{\theta-1} \mathcal{F}(s, x_s)\, ds,$$

we obtain, for $0 \le t_1 < t_2 < T_{\max}$,

$$\begin{aligned} \|x(t_2) - x(t_1)\| &\le \frac{C}{\Gamma(\theta)} \Bigg[\int_0^{t_1} ((t_2 - s)^{\theta-1} - (t_1 - s)^{\theta-1}) ds \\ &\qquad + \int_{t_1}^{t_2} (t_2 - s)^{\theta-1} ds \Bigg] \\ &= \frac{C}{\Gamma(\theta+1)} (t_2^\theta - t_1^\theta) \le \frac{C}{\Gamma(\theta+1)} (t_2 - t_1)^\theta. \end{aligned}$$

Hence, $x(t)$ is uniformly continuous on $[0, T_{\max})$, and the limit

$$x(T_{\max}) := \lim_{t \to T_{\max}^-} x(t)$$

exists. Taking this limit as a new initial history and applying the local existence–uniqueness theorem again, the solution can be extended beyond $T_{\max}$, which contradicts the maximality of $T_{\max}$. Therefore $T_{\max} = +\infty$, and system (3.2) admits a unique continuous solution for all $t \geq 0$. This completes the proof.

Theorem 4.2. (Positivity) All components of the solution remain non-negative for all $t \geq 0$, provided that the initial functions are non-negative on $[-\tau, 0]$.

Proof. Consider our fractional-order delay system written in compact form ${}_0^C D_t^\theta x(t) = f(t, x_t), \quad t \geq 0$, where $x_t \in C([-\tau, 0], \mathbb{R}^5)$ denotes the history segment and $f(t, x_t)$ is the vector-valued function defined in Theorem 4.1, corresponding exactly to the right-hand-sides of system (3.2).

We rely on the invariance criterion of the non-negative cone for Caputo fractional delay differential equations. The non-negative orthant $\mathbb{R}^5_+$ is positively invariant if the following boundary condition holds: for any history function $x_t(\cdot)$ such that $x_t(\nu) \in \mathbb{R}^5_+$ for all $\nu \in [-\tau, 0]$, whenever one state component equals zero and the remaining four components are non-negative at current time t, the corresponding component of vector field $f(t, x_t)$ is non-negative.

Now, we verify the condition for each boundary hyper-surface:

1. If $S(t) = 0$ and $W, F, P, R \geq 0$: The first component of f reads $f_1(t, x_t) = \Pi f(P(t)) \cdot 0 - \alpha_1 \cdot 0 \cdot P - a \cdot 0^2 - \mu \cdot 0 - d \cdot 0 = 0 \geq 0$.

2. If $W(t) = 0$ and all others ≥ 0: $f_2(t, x_t) = \mu S(t) - \alpha_2 \cdot 0 \cdot P - \beta \cdot 0 - d \cdot 0 = \mu S(t) \geq 0$.

3. If $F(t) = 0$ and all others ≥ 0 (note that f_3 depends on the delayed state $F(t - \tau)$ (history value, not current $F(t)$): $f_3(t, x_t) = \alpha_1 S(t) P(t) + \alpha_2 W(t) P(t) - \gamma F(t - \tau) - d \cdot 0$. Here we stress that: the invariance condition for fractional delay systems does not require $f_3 \geq 0$ at the instant t when $F(t) = 0$. Instead, the theorem requires that for all non-negative history functions, solutions cannot depart $\mathbb{R}^5_+$. Since our initial history satisfies $\phi_3(\nu) \geq 0, \nu \in [-\tau, 0]$, and the vector field satisfies the cone-invariance hypothesis for Caputo fractional delay equations, we obtain $F(t) \geq 0$ for all $t \geq 0$.

4. If $P(t) = 0$ and all others ≥ 0: $f_4(t, x_t) = \gamma F(t - \tau) - \eta \cdot 0 - d \cdot 0 = \gamma F(t - \tau) \geq 0$ because $F(t - \tau) \geq 0$ from non-negative history and induction.

5. If $R(t) = 0$ and all others ≥ 0: $f_5(t, x_t) = \eta P(t) + \beta W(t) - d \cdot 0 \geq 0$.

All cone-invariance assumptions are satisfied. Applying the cone invariance result for Caputo fractional delay differential equations, we conclude $S(t) \geq 0$, $W(t) \geq 0$, $F(t) \geq 0$, $P(t) \geq 0$, $R(t) \geq 0$ for all $t \geq 0$. This completes the proof.

Theorem 4.3. (Ultimate boundedness and invariant region) Let

$$\Omega = \left\{ (S, W, F, P, R) \in \mathbb{R}^5_+ : S + W + F + P + R \leq \frac{\Pi^2}{4ad} \right\}.$$

If $N(0) \leq \Pi^2/(4ad)$, then Ω is a positively invariant set. Moreover, all non-negative solutions are uniformly ultimately bounded and satisfy

$$\limsup_{t \to +\infty} N(t) \leq \frac{\Pi^2}{4ad}.$$

Proof. Define $N(t) = S(t) + W(t) + F(t) + P(t) + R(t)$. Summing the five equations of system (3.2), we obtain

$${}_0^C D_t^\theta N(t) = \Pi f(P) S - aS^2 - dN(t).$$

Since $P(t) \geq 0$, we have $0 \leq f(P) \leq 1$. Hence,

$$ {}_0^C D_t^\theta N(t) \leq \Pi S - aS^2 - dN \leq \frac{\Pi^2}{4a} - dN. $$

By the comparison principle for Caputo fractional equations,

$$ N(t) \leq N(0)E_\theta(-dt^\theta) + \frac{\Pi^2}{4ad}(1 - E_\theta(-dt^\theta)). $$

Since $E_\theta(-dt^\theta) \to 0$ as $t \to +\infty$,

$$ \limsup_{t\to+\infty} N(t) \leq \frac{\Pi^2}{4ad}. $$

Moreover, if $N(0) \leq \Pi^2/(4ad)$, then $N(t) \leq \Pi^2/(4ad)$ for all $t \geq 0$. Hence, Ω is positively invariant, and all solutions are uniformly ultimately bounded.

4.2. Existence and stability of the rumor-free equilibrium point E^0

To explore the dynamic evolution characteristics of the fractional-order SWFPR rumor propagation model, obtaining the equilibrium solutions is regarded as a fundamental step for investigating the steady-state properties of the system. On the basis of the constructed system (3.2), the rumor-free equilibrium can be derived as follows:

$$ E^0 = (S_0, W_0, F_0, P_0) = \left(\frac{\Pi - d - \mu}{a}, \frac{(\Pi - d - \mu)\mu}{a(d + \beta)}, 0, 0\right), $$

which is biologically meaningful provided that $\Pi - d - \mu > 0$. First and foremost, we investigate the stability of system (3.2) at the equilibrium point E^0, based on which the following result can be established.

Theorem 4.4. Assume $\Pi - d - \mu > 0$, and define

$$ A_0 = (d + \gamma)(d + \eta) - \gamma(\alpha_1 S_0 + \alpha_2 W_0). $$

Then:

(i) For $\tau = 0$, E^0 is locally asymptotically stable if and only if $A_0 > 0$.

(ii) For $\tau > 0$, E^0 is locally asymptotically stable if and only if every root s of the transcendental equation

$$ (s^\theta + d + \gamma e^{-s\tau})(s^\theta + d + \eta) - \gamma e^{-s\tau}(\alpha_1 S_0 + \alpha_2 W_0) = 0 $$

satisfies $|\arg s| > \theta\pi/2$. If the transcendental equation admits a pair of purely imaginary roots $s = \pm i\omega_0$ at some $\tau_0^0 > 0$ and $\mathrm{Re}(ds/d\tau)|_{\tau=\tau_0^0} \neq 0$, then E^0 loses stability at τ_0^0 and a Hopf bifurcation occurs.

Proof. The rumor-free equilibrium is $E^0 = (S_0, W_0, 0, 0)$, where $S_0 = (\Pi - d - \mu)/a$ and $W_0 = \mu S_0/(\beta + d)$.

Since $\mathcal{L}\{F(t-\tau)\} = e^{-s\tau}\mathcal{L}\{F(t)\}$, the delay factor $e^{-s\tau}$ must be retained in the linearization. The Jacobian matrix of system (3.2) at E^0 is

$$J(E^0) = \begin{pmatrix} -(\Pi - d - \mu) & 0 & 0 & -(\vartheta\Pi + \alpha_1)S_0 \\ \mu & -(\beta + d) & 0 & -\alpha_2 W_0 \\ 0 & 0 & -(d + \gamma e^{-s\tau}) & \alpha_1 S_0 + \alpha_2 W_0 \\ 0 & 0 & \gamma e^{-s\tau} & -(d + \eta) \end{pmatrix}.$$

With $\lambda = s^\theta$, the characteristic matrix is

$$\lambda I - J(E^0) = \begin{pmatrix} \lambda + \Pi - d - \mu & 0 & 0 & (\vartheta\Pi + \alpha_1)S_0 \\ -\mu & \lambda + \beta + d & 0 & \alpha_2 W_0 \\ 0 & 0 & \lambda + d + \gamma e^{-s\tau} & -(\alpha_1 S_0 + \alpha_2 W_0) \\ 0 & 0 & -\gamma e^{-s\tau} & \lambda + d + \eta \end{pmatrix}.$$

Expanding the determinant along the first row, the $(1,4)$-minor vanishes because the first column of the corresponding minor has only one nonzero entry, which is annihilated by the zero entry in the second row. Hence,

$$\det(\lambda I - J(E^0)) = (\lambda + \Pi - d - \mu)(\lambda + \beta + d)\Big[(\lambda + d + \gamma e^{-s\tau})(\lambda + d + \eta) - \gamma e^{-s\tau}(\alpha_1 S_0 + \alpha_2 W_0)\Big],$$

which yields the characteristic equation

$$(\lambda + \Pi - d - \mu)(\lambda + \beta + d)\Big[(\lambda + d + \gamma e^{-s\tau})(\lambda + d + \eta) - \gamma e^{-s\tau}(\alpha_1 S_0 + \alpha_2 W_0)\Big] = 0. \tag{4.1}$$

In what follows, we consider two cases regarding the time delay τ.

(i) $\tau = 0$. Setting $e^{-s\tau} = 1$ in the characteristic equation gives

$$(\lambda + \Pi - d - \mu)(\lambda + \beta + d)[\lambda^2 + (2d + \gamma + \eta)\lambda + A_0] = 0.$$

The first two factors yield

$$\lambda_1 = -(\Pi - d - \mu) < 0, \qquad \lambda_2 = -(\beta + d) < 0.$$

For the quadratic factor, the Routh–Hurwitz criterion gives that both roots have negative real parts if and only if $A_0 > 0$; in that case, they are negative real numbers. Since $\lambda_i < 0$ implies $|\arg(s_i)| = \pi/\theta > \theta\pi/2$ for $\theta \in (0, 1]$, in light of Lemma 2.1, this yields local asymptotic stability of E^0 if and only if $A_0 > 0$.

(ii) $\tau > 0$. The factors $\lambda + \Pi - d - \mu$ and $\lambda + \beta + d$ again give $\lambda_1, \lambda_2 < 0$, which do not affect stability. The remaining roots are determined by the transcendental equation

$$(\lambda + d + \gamma e^{-s\tau})(\lambda + d + \eta) - \gamma e^{-s\tau}(\alpha_1 S_0 + \alpha_2 W_0) = 0,$$

in which the delay factor $e^{-s\tau}$ is retained. By the stability criterion for fractional-order delay differential equations, E^0 is locally asymptotically stable if and only if every root s satisfies $|\arg s| > \theta\pi/2$. If a pair of purely imaginary roots $s = \pm i\omega_0$ appears at $\tau = \tau_0^0$ and the transversality condition holds, then the roots cross the imaginary axis and E^0 loses stability through a Hopf bifurcation at τ_0^0. When $A_0 > 0$, continuity ensures that the transcendental equation has no root on the imaginary axis for sufficiently small $\tau > 0$, so E^0 remains stable on $[0, \tau_0^0)$.

4.3. Existence and stability of the endemic rumor equilibrium E^*

Set

$$S_0 = \frac{\Pi - d - \mu}{a}, \qquad W_0 = \frac{\mu S_0}{d+\beta},$$

and

$$D_0 := \frac{\gamma(\alpha_1 S_0 + \alpha_2 W_0)}{(d+\gamma)(d+\eta)}.$$

When $\alpha_2 = \alpha_1$, this reduces to

$$D_0 = \frac{\gamma\alpha_1 S_0(d+\beta+\mu)}{(d+\gamma)(d+\eta)(d+\beta)}.$$

Substituting the endemic expressions

$$S^* = \frac{(d+\gamma)(d+\eta)(d+\alpha_1 P^*+\beta)}{\gamma\alpha_1(d+\alpha_1 P^*+\beta+\mu)}, \quad W^* = \frac{\mu S^*}{d+\alpha_1 P^*+\beta}, \quad F^* = \frac{d+\eta}{\gamma}P^*$$

into the S-equation yields the cubic equation

$$\mathcal{P}(P) := AP^3 + BP^2 + CP + D = 0, \tag{4.2}$$

where

$$\begin{aligned}
A &= \gamma\alpha_1^3\vartheta,\\
B &= \gamma\alpha_1^2(d+\mu)\vartheta + \gamma\alpha_1^2 + a(d+\gamma)(d+\eta)\alpha_1\vartheta,\\
C &= \Pi\gamma\alpha_1^2 - \gamma\alpha_1(d+\mu)^2\vartheta - \gamma\alpha_1(d+\mu) + \gamma\alpha_1^2\vartheta(d+\mu+\beta)\\
&\quad + a(d+\gamma)(d+\eta)\left[\alpha_1 + \vartheta(d+\beta)\right].
\end{aligned}$$

A direct computation gives

$$D = a(d+\gamma)(d+\eta)(d+\beta)\,(D_0 - 1). \tag{4.3}$$

Consequently,

$$D < 0 \iff D_0 > 1.$$

Lemma 4.1. If $\alpha_2 = \alpha_1$ and $D_0 > 1$ (equivalently, $D < 0$), then system (3.2) admits a unique positive endemic equilibrium $E^* = (S^*, W^*, F^*, P^*)$ and P^* is the unique positive root of system (4.2).

Proof. Existence. Since $A > 0$, $\mathcal{P}(P) \to +\infty$ as $P \to +\infty$. By Eq (4.3), $D < 0$, so $\mathcal{P}(0) = D < 0$. By the intermediate value theorem, there exists $P^* > 0$ with $\mathcal{P}(P^*) = 0$. Substituting P^* into the expressions for S^*, W^*, F^* gives $S^*, W^*, F^* > 0$, and these values satisfy the S-equation by construction. Hence E^* is a positive equilibrium.

Uniqueness. Since $A > 0$ and $B > 0$, and $D < 0$, the coefficient sequence (A, B, C, D) has signs $(+, +, \operatorname{sgn} C, -)$, regardless of the sign of C. In all three cases $C > 0$, $C = 0$, $C < 0$, the number of sign changes is exactly one. By Descartes' rule of signs, $\mathcal{P}(P)$ has exactly one positive root, counted with multiplicity. Combined with existence, the positive root is unique.

Remark 2. The condition $D < 0$ is sufficient but not necessary for the existence of a positive endemic equilibrium. If $D \geq 0$ and $C < 0$, the sign sequence $(+, +, -, +)$ has two sign changes, and $\mathcal{P}(P)$ may possess two positive roots. Therefore the original statement "E^* exists if and only if $D < 0$" should be read as "E^* exists and is unique if $D < 0$". If one wishes to retain an "if and only if" statement, the additional assumption $C \geq 0$ is required; under this assumption, $D \geq 0$ gives the sign sequence $(+, +, +, +)$ with no sign change, so no positive root exists, and hence

$$E^* \text{ exists} \iff D < 0 \iff D_0 > 1.$$

Within the framework of this subsection, we set $\tau = 0$. In Subsection 4.4, the parameter τ is chosen as the bifurcation parameter, which serves to locate the bifurcation points of system (3.2) and yield the corresponding conditions for Hopf bifurcation.

At the equilibrium point E^*, the linearized form corresponding to system (3.2) is obtainable through the methodology presented as follows:

Let $\bar{S}(t) = S(t) - S^*$, $\bar{W}(t) = W(t) - W^*$, $\bar{F}(t) = F(t) - F^*$, $\bar{P}(t) = P(t) - P^*$, $\bar{R}(t) = R(t) - R^*$. The linear system of system (3.2) is

$$\begin{cases} {}_0^C D_t^\theta \bar{S}(t) = \left(\dfrac{\Pi}{1+\vartheta P^*} - \alpha_1 P^* - 2aS^* - \mu - d\right)\bar{S}(t) \\ \qquad\qquad + \left(-\dfrac{\Pi\vartheta S^*}{(1+\vartheta P^*)^2} - \alpha_1 S^*\right)\bar{P}(t), \\ {}_0^C D_t^\theta \bar{W}(t) = \mu\bar{S}(t) - (\alpha_2 P^* + \beta + d)\,\bar{W}(t) - \alpha_2 W^* \bar{P}(t), \\ {}_0^C D_t^\theta \bar{F}(t) = \alpha_1 P^* \bar{S}(t) + \alpha_2 P^* \bar{W}(t) + (\alpha_1 S^* + \alpha_2 W^*)\,\bar{P}(t) \\ \qquad\qquad - d\bar{F}(t) - \gamma\bar{F}(t), \\ {}_0^C D_t^\theta \bar{P}(t) = \gamma\bar{F}(t) - (\eta + d)\bar{P}(t), \\ {}_0^C D_t^\theta \bar{R}(t) = \beta\bar{W}(t) + \eta\bar{P}(t) - d\bar{R}(t). \end{cases} \tag{4.4}$$

It is worth noting that $\bar{R}(t)$ has no interdependence with the first three parts of system (4.3), thereby enabling us to investigate the subsequent subsystem:

$$\begin{cases} {}_0^C D_t^\theta \bar{S}(t) = \left(\dfrac{\Pi}{1+\vartheta P^*} - \alpha_1 P^* - 2aS^* - \mu - d\right)\bar{S}(t) \\ \qquad\qquad + \left(-\dfrac{\Pi\vartheta S^*}{(1+\vartheta P^*)^2} - \alpha_1 S^*\right)\bar{P}(t), \\ {}_0^C D_t^\theta \bar{W}(t) = \mu\bar{S}(t) - (\alpha_2 P^* + \beta + d)\,\bar{W}(t) - \alpha_2 W^* \bar{P}(t), \\ {}_0^C D_t^\theta \bar{F}(t) = \alpha_1 P^* \bar{S}(t) + \alpha_2 P^* \bar{W}(t) + (\alpha_1 S^* + \alpha_2 W^*)\,\bar{P}(t) \\ \qquad\qquad - d\bar{F}(t) - \gamma\bar{F}(t), \\ {}_0^C D_t^\theta \bar{P}(t) = \gamma\bar{F}(t) - (\eta + d)\bar{P}(t). \end{cases} \tag{4.5}$$

Applying the Laplace transform to the above system and utilizing Lemma 2.2, the characteristic equation of the linearized system (4.4) is derived with the aid of Lemma 2.3, as given below:

$$\Delta(s) = \begin{pmatrix} s^\theta - c_{11} & 0 & 0 & c_{14} \\ -c_{21} & s^\theta - c_{22} & 0 & c_{24} \\ c_{31} & c_{32} & s^\theta + d + \gamma & c_{34} \\ 0 & 0 & -\gamma & s^\theta + c_{44} \end{pmatrix}, \tag{4.6}$$

where

$$\begin{aligned} c_{11} &= \frac{\Pi}{1+\vartheta P^*} - \alpha_1 P^* - d - 2aS^* - \mu, \\ c_{14} &= -\frac{\Pi\vartheta S^*}{(1+\vartheta P^*)^2} - \alpha_1 S^*, \\ c_{21} &= \mu, \\ c_{22} &= \alpha_2 P^* + \beta + d, \\ c_{24} &= -\alpha_2 W^*, \\ c_{31} &= \alpha_1 P^*, \\ c_{32} &= \alpha_2 P^*, \\ c_{34} &= \alpha_1 S^* + \alpha_2 W^*, \\ c_{44} &= d + \eta. \end{aligned}$$

Accordingly, the characteristic equation of the linearized system (4.4) corresponding to system (3.2) can be characterized in the form of a matrix determinant, i.e.,

$$\det(\Delta(s)) = \begin{vmatrix} s^\theta - c_{11} & 0 & 0 & c_{14} \\ -c_{21} & s^\theta - c_{22} & 0 & c_{24} \\ c_{31} & c_{32} & s^\theta + d + \gamma & c_{34} \\ 0 & 0 & -\gamma & s^\theta + c_{44} \end{vmatrix} = 0. \tag{4.7}$$

This characteristic equation (denoted as Eq (4.2)) serves as a core tool for analyzing the dynamic properties of system (3.2). If all the roots of characteristic equation (4.2) satisfy the condition that their real parts are less than zero, then system (3.2) possesses local asymptotic stability at the positive equilibrium point P^*, whereas if there exists at least one root with a positive real part in characteristic equation (4.2), system (3.2) loses stability at the positive equilibrium point P^*.

Furthermore, when a time delay is introduced to modify system (3.2), the corresponding characteristic equation (denoted as Eq (4.7)) can be transformed into the following form:

$$M_1(\lambda) + M_2(\lambda) = 0, \tag{4.8}$$

where $\lambda = s^\theta$,

$$\begin{aligned} M_1(\lambda) &= \lambda^4 + M_{13}\lambda^3 + M_{12}\lambda^2 + M_{11}\lambda + M_{10}, \\ M_2(\lambda) &= M_{23}\lambda^3 + M_{22}\lambda^2 + M_{21}\lambda + M_{20}, \end{aligned}$$

where

$$M_{13} = d - c_{11} - c_{22} + c_{44},$$

$$
\begin{aligned}
M_{12} &= -d(c_{11}+c_{22}) + c_{11}c_{22} + c_{44}(d - c_{11} - c_{22}),\\
M_{11} &= c_{44}(-d(c_{11}+c_{22}) + c_{11}c_{22}) + d\,c_{11}c_{22},\\
M_{10} &= c_{44}\,d\,c_{11}c_{22},\\
M_{23} &= -\gamma,\\
M_{22} &= \gamma(c_{11}+c_{22}-(c_{44}+c_{34})),\\
M_{21} &= -\gamma\Big\{-c_{11}c_{22} - (c_{11}+c_{22})(c_{44}+c_{34}) + c_{14}c_{31}\Big\},\\
M_{20} &= -\gamma\Big\{c_{11}c_{22}(c_{44}+c_{34}) + c_{14}c_{21}c_{32} - c_{14}c_{31}c_{22}\Big\}.
\end{aligned}
$$

When the system is free of time delay (i.e., $\tau = 0$), characteristic equation (4.7) corresponding to the fractional-order rumor propagation model is transformed into the following form:

$$M_1(s) + M_2(s) = 0.$$

Subsequently, by introducing the substitution $s^\theta = \xi$, the following expression can be derived:

$$K_{14}\xi^4 + K_{13}\xi^3 + K_{12}\xi^2 + K_{11}\xi + K_{10} = 0, \tag{4.9}$$

where

$$
\begin{aligned}
K_{14} &= 1,\\
K_{13} &= M_{13} + M_{23},\\
K_{12} &= M_{12} + M_{22},\\
K_{11} &= M_{11} + M_{21},\\
K_{10} &= M_{10} + M_{20}.
\end{aligned}
$$

Corresponding to characteristic equation (4.8), the Hurwitz determinant

$$\Delta = \begin{vmatrix} K_{13} & 1 & 0 & 0\\ K_{11} & K_{12} & K_{13} & 1\\ 0 & K_{10} & K_{11} & K_{12}\\ 0 & 0 & 0 & K_{10}\end{vmatrix}.$$

Assumption 1. The system (3.2) is locally asymptotically stable at the positive equilibrium point E^* if the polynomial corresponding to characteristic equation (4.8) satisfies the following conditions:

(i) Strict positivity of coefficients: $M_{13} > 0, M_{12} > 0, M_{11} > 0, M_{10} > 0$;
(ii) Strict positivity of Hurwitz leading principal minors: $\Delta_1 = M_{12} > 0$, $\Delta_2 = M_{12}M_{11} - M_{13}M_{10} > 0$, $\Delta_3 = M_{10}\Delta_2 > 0$.

Theorem 4.5. If $\alpha_2 = \alpha_1$, $D_0 > 1$, and $\tau = 0$, the fractional-order satisfies $\theta \in (0, 1]$, and the conditions of Assumption 1 hold. Then, the unique positive equilibrium point E^* of system (3.2) is locally asymptotically stable.

Proof. When $\tau = 0$ (i.e., the time delay effect vanishes), characteristic equation (4.8) can be simplified to the factored form $(\xi - r_1)(\xi - r_2)(\xi - r_3)(\xi - r_4) = 0$, where $\xi_1, \xi_2, \xi_3, \xi_4$ denote the four characteristic

roots of Eq (4.8). If all conditions of Assumption 1 are satisfied, it can be determined by the Routh–Hurwitz stability criterion that all roots of characteristic equation (4.8) have strictly negative real parts. Further, combined with the conclusion in Lemma 2.1 that "all roots with negative real parts imply local asymptotic stability of the system equilibrium", it can be deduced that the positive equilibrium point E^* of system (3.2) is locally asymptotically stable.

4.4. Time-delay critical threshold and Hopf bifurcation

Next, we discuss the case where the time delay parameter satisfies $\tau > 0$. Set $s = i\varpi = \varpi e^{\frac{\pi i}{2}} = \varpi\left(\cos\frac{\pi}{2} + i\sin\frac{\pi}{2}\right)$, and we thus derive that

$$(\cos\varpi\tau - i\sin\varpi\tau) = -\frac{M_1(i\varpi)}{M_2(i\varpi)}, \quad M_2(i\varpi) \neq 0, \tau > 0.$$

By decomposing the aforementioned equation into its real and imaginary components, we derive

$$\cos\varpi\tau = -\frac{AX + BY}{X^2 + Y^2},$$

$$\sin\varpi\tau = \frac{BX - AY}{X^2 + Y^2}.$$

At this point,

$$\begin{aligned}
A &= \mathrm{Re}\,[M_1(i\varpi)] = M_{14}\varpi^{4\theta}\cos 2\pi\theta + M_{13}\varpi^{3\theta}\cos\frac{3\pi\theta}{2} \\
&\quad + M_{12}\varpi^{2\theta}\cos\pi\theta + M_{11}\varpi^{\theta}\cos\frac{\pi\theta}{2} + M_{10}, \\
B &= \mathrm{Im}\,[M_1(i\varpi)] = M_{14}\varpi^{4\theta}\sin 2\pi\theta + M_{13}\varpi^{3\theta}\sin\frac{3\pi\theta}{2} \\
&\quad + M_{12}\varpi^{2\theta}\sin\pi\theta + M_{11}\varpi^{\theta}\sin\frac{\pi\theta}{2}, \\
X &= \mathrm{Re}\,[M_2(i\varpi)] = M_{23}\varpi^{3\theta}\cos\frac{3\pi\theta}{2} + M_{22}\varpi^{2\theta}\cos\pi\theta \\
&\quad + M_{21}\varpi^{\theta}\cos\frac{\pi\theta}{2} + M_{20}, \\
Y &= \mathrm{Im}\,[M_2(i\varpi)] = M_{23}\varpi^{3\theta}\sin\frac{3\pi\theta}{2} + M_{22}\varpi^{2\theta}\sin\pi\theta + M_{21}\varpi^{\theta}\sin\frac{\pi\theta}{2}.
\end{aligned}$$

By virtue of the fundamental trigonometric identity $\cos^2(\varpi\tau) + \sin^2(\varpi\tau) = 1$, we arrive at the following:

$$\begin{aligned}
&\varpi^{8\theta} + g_7\varpi^{7\theta} + g_6\varpi^{6\theta} + g_5\varpi^{5\theta} + g_4\varpi^{4\theta} \\
&\quad + g_3\varpi^{3\theta} + g_2\varpi^{2\theta} + g_1\varpi^{\theta} + g_0 = 0,
\end{aligned} \tag{4.10}$$

where

$$\begin{aligned}
g_7 &= 2M_{13}\cos 2\pi\theta\cos\frac{3\pi\theta}{2} + 2M_{13}\sin 2\pi\theta\sin\frac{3\pi\theta}{2}, \\
g_6 &= M_{13}^2 + 2M_{12}\cos 2\pi\theta\cos\pi\theta
\end{aligned}$$

$$
\begin{aligned}
&+ 2M_{12}\sin 2\pi\theta \sin \pi\theta - M_{23}^2,\\
g_5 &= 2M_{11}\cos 2\pi\theta \cos\frac{\pi\theta}{2} + 2M_{13}M_{12}\cos\frac{3\pi\theta}{2}\cos\pi\theta\\
&+ 2M_{11}\sin 2\pi\theta \sin\frac{\pi\theta}{2} + 2M_{13}M_{12}\sin\frac{3\pi\theta}{2}\sin\pi\theta\\
&- 2M_{23}M_{22}\cos\frac{3\pi\theta}{2}\cos\pi\theta - 2M_{23}M_{22}\sin\frac{3\pi\theta}{2}\sin\pi\theta,\\
g_4 &= M_{12}^2 - M_{22}^2 + 2M_{10}\cos 2\pi\theta + 2M_{13}M_{11}\cos\frac{3\pi\theta}{2}\cos\frac{\pi\theta}{2}\\
&+ 2M_{13}M_{11}\sin\frac{3\pi\theta}{2}\sin\frac{\pi\theta}{2} - 2M_{23}M_{21}\cos\frac{3\pi\theta}{2}\cos\frac{\pi\theta}{2},\\
g_3 &= 2M_{13}M_{10}\cos\frac{3\pi\theta}{2} + 2M_{12}M_{11}\cos\pi\theta\cos\frac{\pi\theta}{2}\\
&+ 2M_{12}M_{11}\sin\pi\theta\sin\frac{\pi\theta}{2} - 2M_{23}M_{20}\cos\frac{3\pi\theta}{2}\\
&- 2M_{22}M_{21}\cos\pi\theta\cos\frac{\pi\theta}{2},\\
g_2 &= M_{11}^2 - M_{21}^2 + 2M_{12}M_{10}\cos\pi\theta - 2M_{22}M_{20}\cos\pi\theta,\\
g_1 &= 2M_{11}M_{10}\cos\frac{\pi\theta}{2} - 2M_{21}M_{20}\cos\frac{\pi\theta}{2},\\
g_0 &= M_{10}^2 - M_{20}^2.
\end{aligned}
$$

Subsequently, characteristic equation (4.10) is further simplified. By introducing the variable substitution $\ell = \varpi^{\theta}$ (where ℓ denotes a newly defined auxiliary variable), we can derive the following result:

$$\psi(\ell) = \ell^8 + g_7\ell^7 + g_6\ell^6 + g_5\ell^5 + g_4\ell^4 + g_3\ell^3 + g_2\ell^2 + g_1\ell + g_0. \tag{4.11}$$

Take the derivative of both sides of Eq (4.11):

$$\psi'(\ell) = 8\ell^7 + 7g_7\ell^6 + 6g_6\ell^5 + 5g_5\ell^4 + 4g_4\ell^3 + 3g_3\ell^2 + 2g_2\ell + g_1. \tag{4.12}$$

Assumption 2. $g_0 < 0$.

Theorem 4.6. From characteristic equation (4.11), the following key inferences can be drawn:

(i) No positive real roots exist for characteristic equation (4.11) under the condition that all its coefficients satisfy $g_i \geq 0$ $(i = 0, 1, \ldots, 7)$;

(ii) When Assumption 2 is satisfied, characteristic equation (4.11) possesses at least one positive root ξ_0, which in turn implies that the original characteristic equation (4.11) has one pair of purely imaginary roots.

Proof. (i) Under the constraint of non-negative coefficients $g_i \geq 0$ $(i = 0, 1, \ldots, 7)$, a critical premise for this analysis find is that the derivative $\psi'(\ell) > 0$ for all positive values of ξ. This derivative property confirms that $\psi(\ell)$ exhibits strict monotonic increase on the interval $\ell > 0$. Moreover, since the function value at zero satisfies $\psi(0) = g_0 \geq 0$, we can directly conclude that characteristic equation (4.11) lacks any positive real roots.

(ii) First, the continuity of $\psi(\ell)$ across its entire domain is self-evident. When combined with the boundary conditions $\psi(0) = g_0 < 0$ and $\psi(+\infty) > 0$, the zero-point theorem ensures the existence of at least one positive root ℓ_0 for characteristic equation (4.11). As a direct consequence, Eq (4.10) has a positive root $\varpi_0 = \sqrt[\theta]{\ell_0}$, leading to the conclusion that the original characteristic equation (4.10) contains at least one pair of purely imaginary roots $\pm i\varpi_0$. □

Now we discuss the Hopf bifurcation of system (3.2).

Assumption 3. $m_1n_1 + m_2n_2 > 0$.

Lemma 4.2. If Assumption 3 holds, then:

(1) Let ℓ_0 be a positive real root of the polynomial $\psi(\ell) = 0$, and define the corresponding imaginary part coefficient as $\varpi_0 = \ell_0^{1/\theta}$. Substituting ϖ_0 back into the real and imaginary part expressions of Eq (4.11), the sequence of critical time delay values can be obtained as:

$$\tau_0^{(k)} = \frac{1}{\varpi_0}\left[\arccos\left(\frac{-(AX + BY)}{X^2 + Y^2}\right) + 2k\pi\right], \quad k = 0, 1, 2, \ldots,$$

where τ_0 denotes the minimum positive critical value in the sequence;

(2) Let $L(\tau) = p(\tau) + i\varpi(\tau)$ be a root of Eq (4.10) near $\tau = \tau_0$ satisfying $p(\tau_0) = 0$ and $\varpi(\tau_0) = \varpi_0$ (with $\varpi_0 > 0$ being a constant). Then the transversality condition:

$$\mathrm{Re}\left(\frac{ds}{d\tau}\right)\Big|_{\tau=\tau_0} > 0$$

holds.

Proof. First, we derive the critical time delay sequence: relying on the 2π-periodicity of the cosine function ($\cos \varpi_0\tau = \cos(\varpi_0\tau + 2k\pi)$), the sequence $\tau_0^{(k)}$ (as given in part (1)) is constructed. To ensure the physical significance of the time delay, we select the smallest positive term from this sequence as the bifurcation critical point: $\tau_0 = \min\left\{\tau_0^{(k)} \mid k = 0, 1, 2, \ldots\right\} = \tau_0^{(0)}$.

Next, we verify the transversality condition (a necessary criterion for Hopf bifurcation) by analyzing the derivative of the characteristic root with respect to τ: We differentiate both sides of the characteristic equation (4.8) with respect to τ. For the time-delay term $e^{-s\tau}$ in the equation, we apply the product rule of differentiation (combining the derivative of the exponential function and the chain rule). After rearranging terms related to $\frac{ds}{d\tau}$, we obtain:

$$\left(\frac{ds}{d\tau}\right)^{-1} = \frac{M_1'(s)e^{s\tau} + M_2'(s)}{sM_2(s)} - \frac{\tau}{s}. \tag{4.13}$$

Here, $M_1(s)$ and $M_2(s)$ are the two polynomial sub-terms decomposed from Eq (4.8), which correspond to the non-time-delay and time-delay parts of the characteristic equation, respectively.

We substitute the critical values $\tau = \tau_0$ and $s = i\varpi_0$ (noting that $p(\tau_0) = 0$ implies the root is purely imaginary at τ_0) into Eq (4.9). By simplifying the complex arithmetic (separating real and imaginary parts of the exponential term $e^{i\varpi_0\tau_0}$), we get:

$$\left(\frac{ds}{d\tau}\right)^{-1} = \frac{im_1 + m_2}{in_1 + n_2} - \frac{\tau_0}{i\varpi_0}, \tag{4.14}$$

where the coefficients are redefined based on the real/imaginary parts of $M_1'(i\varpi_0)$ and $M_2(i\varpi_0)$:

$$\begin{aligned} m_1 &= \mathrm{Re}\left[M_1'(i\varpi_0)\right]\sin(\varpi_0\tau_0) + \mathrm{Im}\left[M_2(i\varpi_0)\right] \\ &\quad + \mathrm{Im}\left[M_1'(i\varpi_0)\right]\cos(\varpi_0\tau_0), \\ m_2 &= \mathrm{Re}\left[M_1'(i\varpi_0)\right]\cos(\varpi_0\tau_0) + \mathrm{Re}\left[M_2(i\varpi_0)\right] \\ &\quad - \mathrm{Im}\left[M_1'(i\varpi_0)\right]\sin(\varpi_0\tau_0), \\ n_1 &= \varpi_0 \cdot \mathrm{Re}\left[M_2(i\varpi_0)\right], \\ n_2 &= -\varpi_0 \cdot \mathrm{Im}\left[M_2(i\varpi_0)\right]. \end{aligned}$$

To determine the sign of $\mathrm{Re}\left(\frac{ds}{d\tau}\right)\Big|_{\tau=\tau_0}$, we calculate the real part of Eq (4.10). Using the property that $\mathrm{Re}(z^{-1}) = \mathrm{Re}(z)/|z|^2$ for complex $z \neq 0$, we simplify to:

$$\mathrm{Re}\left(\frac{ds}{d\tau}\right)^{-1} = \frac{m_1 n_1 + m_2 n_2}{n_1^2 + n_2^2}. \tag{4.15}$$

From Assumption 3, the numerator $m_1 n_1 + m_2 n_2$ is strictly positive. Since the denominator $n_1^2 + n_2^2$ is a sum of squares (thus, positive-definite), we conclude that $\mathrm{Re}\left(\frac{ds}{d\tau}\right)\Big|_{\tau=\tau_0} > 0$. This satisfies the transversality condition, and the proof of Lemma 4.2 is thus complete.

In summary, the following main conclusions can be drawn:

Theorem 4.7. Provided that Assumptions 1 through 3 hold simultaneously, the following results can be inferred:

(i) For the time-delay range $\tau \in [0, \tau_0)$, the positive equilibrium point E^* of system (3.2) is locally asymptotically stable;

(ii) At the critical time delay $\tau = \tau_0$, a Hopf bifurcation emerges at the positive equilibrium point E^* of system (3.2);

(iii) When the time delay exceeds the critical value (i.e., $\tau \in (\tau_0, +\infty)$), the positive equilibrium point E^* of system (3.2) loses its stability completely.

5. Numerical simulations

To further elaborate on the theoretical findings of this paper and verify their validity and feasibility, numerical simulation studies are conducted in this section. Two classes of parameter values are adopted in the numerical simulations. The baseline parameters in Table 1 are mainly referenced from existing rumor propagation models for online social networks. Some parameters, such as α_1 in Table 2 and the fear-factor values in Section 4.2, are tuned to explore different dynamical regimes and bifurcation scenarios. These tuned values are not empirical fitted estimate because reliable real-world quantitative measurements for fear-response coefficients in online rumor spreading are still limited in the available literature. The numerical results serve to illustrate qualitative dynamical behaviors rather than to provide precise quantitative predictions for a specific social platform.

The Caputo fractional delayed system is solved using the predictor-corrector Predict, Evaluate, Correct, Evaluate (PECE) (Adams–Bashforth–Moulton) scheme for fractional delay differential equations. A uniform time step $h = 0.01$ is used for all primary numerical runs. For the delayed term $F(t - \tau)$, linear interpolation is applied to approximate state values at off-grid points. The history

function on $[-\tau, 0]$ is constant: $S(t) = S_0$, $W(t) = W_0$, $F(t) = F_0$, $P(t) = P_0$, $R(t) = R_0$, where $(S_0, W_0, F_0, P_0, R_0)$ are the initial states. A step-size convergence test is conducted near the Hopf bifurcation critical value by reducing h to 0.005 and 0.0025. The equilibrium, bifurcation threshold, and periodic orbit amplitude show negligible variation, verifying the numerical reliability.

5.1. Stability of equilibrium points

In this section, we discuss the stability of the rumor-free equilibrium E^0 and the endemic rumor equilibrium E^*, respectively. The initial values are set as $S_0 = 2500$, $W_0 = 120$, $F_0 = 100$, and $P_0 = 50$.

Table 1. Parameter values.

Parameter	Description	Value
Π	Immigration rate	0.0333
d	Natural exit rate for all populations	3.3×10^{-5}
a	Intraspecific competition rate	0.0000037
ϑ	Fear factor	5×10^{-5}
α_1	Transmission rate	2×10^{-6}
β	Official rumor refutation rate	0.02097
γ	Conversion rate from F to P	0.1
η	Spontaneous recovery rate of propagators	0.05
μ	Transition rate from S to W	0.0267
τ	Time delay	1

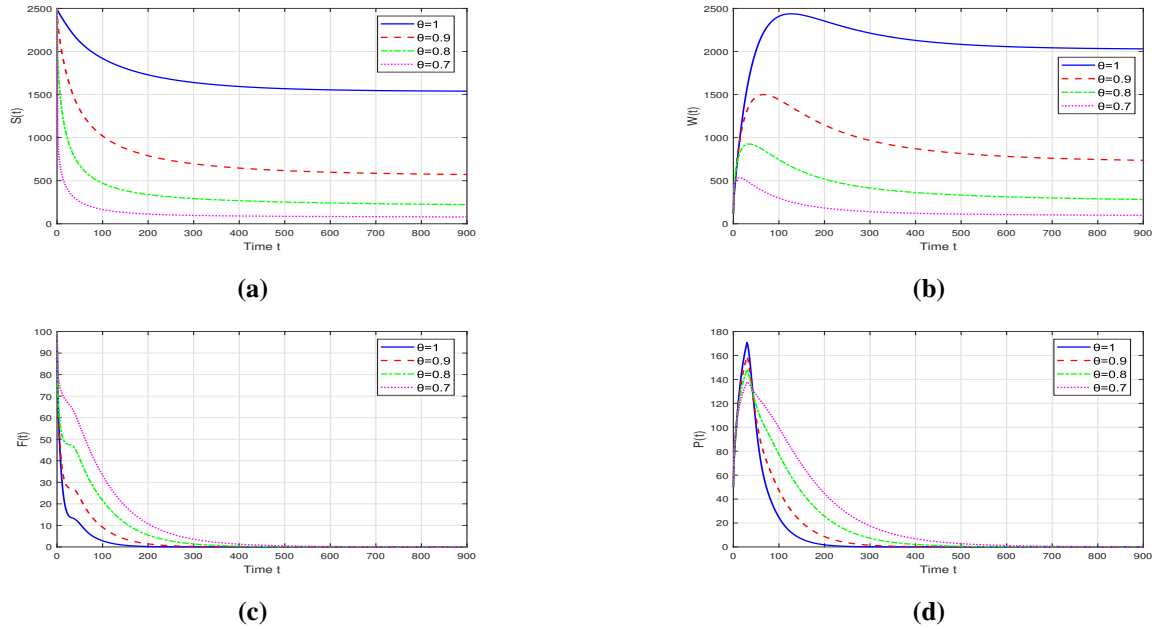

Figure 2. Local asymptotic stability of E^0 in system (3.2) with $\theta = 1$, $\theta = 0.9$, $\theta = 0.8$, and $\theta = 0.7$. Panels (a)–(d) show the convergence of $S(t)$, $W(t)$, $F(t)$, and $P(t)$ to the equilibrium E^0, illustrating the local asymptotic stability of E^0 for $\theta = 1$, 0.9, 0.8, and 0.7, respectively.

Example 1. First, the parameters presented in Table 1 are imported into dynamical system (3.2). Numerical simulations are carried out and the corresponding outcomes are plotted in Figure 2. This figure depicts the time-dependent evolutionary profiles of the population density in each compartment under four distinct fractional orders, namely, $\theta = 1$, $\theta = 0.9$, $\theta = 0.8$, and $\theta = 0.7$.

It can be clearly observed from Figure 2(a)–(d) that the convergence speed of solutions to system (3.2) gradually decelerates as the fractional order declines. Meanwhile, the time cost for the disease-free equilibrium to realize asymptotic stability is extended with the reduction of the fractional order. On this basis, it can be inferred that the disease-free equilibrium E^0 remains globally asymptotically stable within the aforementioned interval of fractional orders.

Table 2. Parameter values.

Parameter	Description	Value
Π	Immigration rate	0.0333
d	Natural exit rate for all populations	3.3×10^{-5}
a	Intraspecific competition rate	0.0000037
ϑ	Fear factor	5×10^{-5}
α_1	Transmission rate	2.67×10^{-6}
β	Official rumor refutation rate	0.02097
γ	Conversion rate from F to P	0.1
η	Spontaneous recovery rate of propagators	0.05
μ	Transition rate from S to W	0.0267
τ	Time delay	1

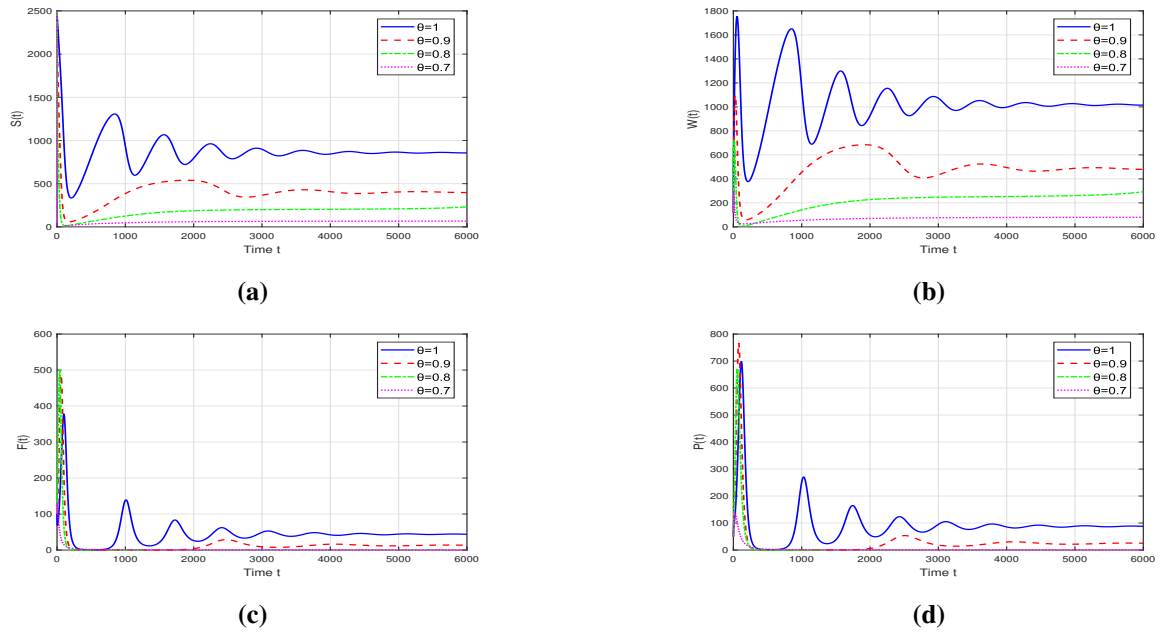

Figure 3. Local asymptotic stability of E^* in system (3.2) with $\theta = 1$, $\theta = 0.9$, $\theta = 0.8$, and $\theta = 0.7$. Panels (a)–(d) show the convergence of $S(t)$, $W(t)$, $F(t)$, and $P(t)$ to the equilibrium E^* , illustrating the local asymptotic stability of E^* for $\theta = 1$, 0.9, 0.8, and 0.7, respectively.

Example 2. Subsequently, another group of parametric values listed in Table 2 is adopted and substituted into system (3.2). Through strict mathematical derivation, the rumor-endemic equilibrium of the dynamical system is obtained. In line with the theoretical conclusion given in Theorem 4.5, the rumor-endemic equilibrium E^* is thereby verified to be locally asymptotically stable, which implies that rumors can maintain long-term persistence within the social system.

Corresponding numerical simulations are displayed in Figure 3(a)–(d), where the evolutionary trends of each subpopulation are described under four fractional orders $\theta = 1$, $\theta = 0.9$, $\theta = 0.8$, and $\theta = 0.7$, respectively. It can be further observed that the peak density of each compartment declines monotonically as the fractional order decreases.

5.2. The effects of the fear factor on rumor propagation ϑ

This study focuses on examining how the fear coefficient affects the evolutionary dynamics of rumor propagation. Under the condition that all other parameters remain unchanged and $\alpha_1 = 2.67 \times 10^{-5}$, the system possesses a unique rumor-endemic equilibrium E^*. Figure 4(a)–(d) depicts the dynamical evolution profiles of $P(t)$ with various combinations of fear factors $\vartheta = 0.00005, 0.0005, 0.00089, 0.05$ and fractional orders $\theta = 1, 0.9, 0.8, 0.7$.

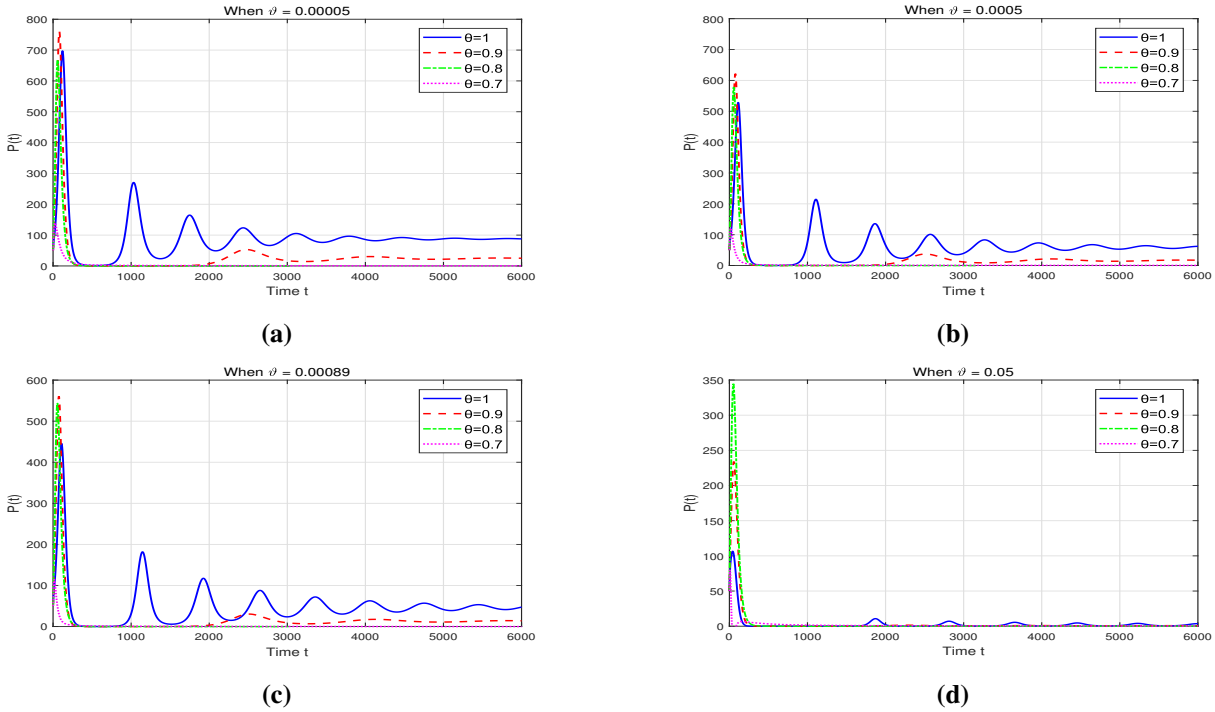

Figure 4. Dynamical evolution profiles of $P(t)$ under various combinations of fear factors $\vartheta = 0.00005, 0.0005, 0.00089, 0.05$ and fractional orders $\theta = 1, 0.9, 0.8, 0.7$, where panels (a)–(d) show the convergence of $P(t)$ for these parameter sets, respectively.

Quantitative investigations based on the numerical outcomes shown in Figure 4(a)–(d) reveal that an increasing fear coefficient generates a continuous inhibitory effect on the density of rumor-spreading individuals within the system. Specifically, a higher fear factor not only suppresses the peak scale of rumor propagation, but also significantly shortens the attenuation period of the

spreading population. Such evolutionary characteristics demonstrate the behavioral regulatory function induced by fear, which encourages the public to take proactive defensive measures, such as reducing social contact, to lower the risk of exposure to rumors.

Therefore, the fear triggered by rumor transmission acts as a critical regulatory factor governing the dynamic evolution of rumors and provides an essential theoretical basis for rumor governance. In practical applications, scientific and targeted risk communication measures, such as precise rumor-refuting strategies, can effectively enhance the efficiency of rumor suppression. Nevertheless, the intensity and frequency of such interventions should be reasonably controlled to prevent excessive intervention from triggering adverse psychosocial reactions and undermining the stability of public governance.

5.3. The effects of official rumor-refuting rate β

Under the condition that all other parameters remained unchanged, this study investigated the regulatory mechanism of official rumor-refuting behavior in the dynamic evolution of rumor propagation. Numerical simulations were conducted using the benchmark parameters listed in Table 2, where the rumor transmission rate was set to 8×10^{-4}. Figure 5(a)–(d) shows the temporal evolution of the rumor propagator density $P(t)$ corresponding to different official rumor-refuting rates $\beta = 0.085, 0.255, 0.455, 0.625$ and fractional orders $\theta = 1, 0.9, 0.8, 0.7$.

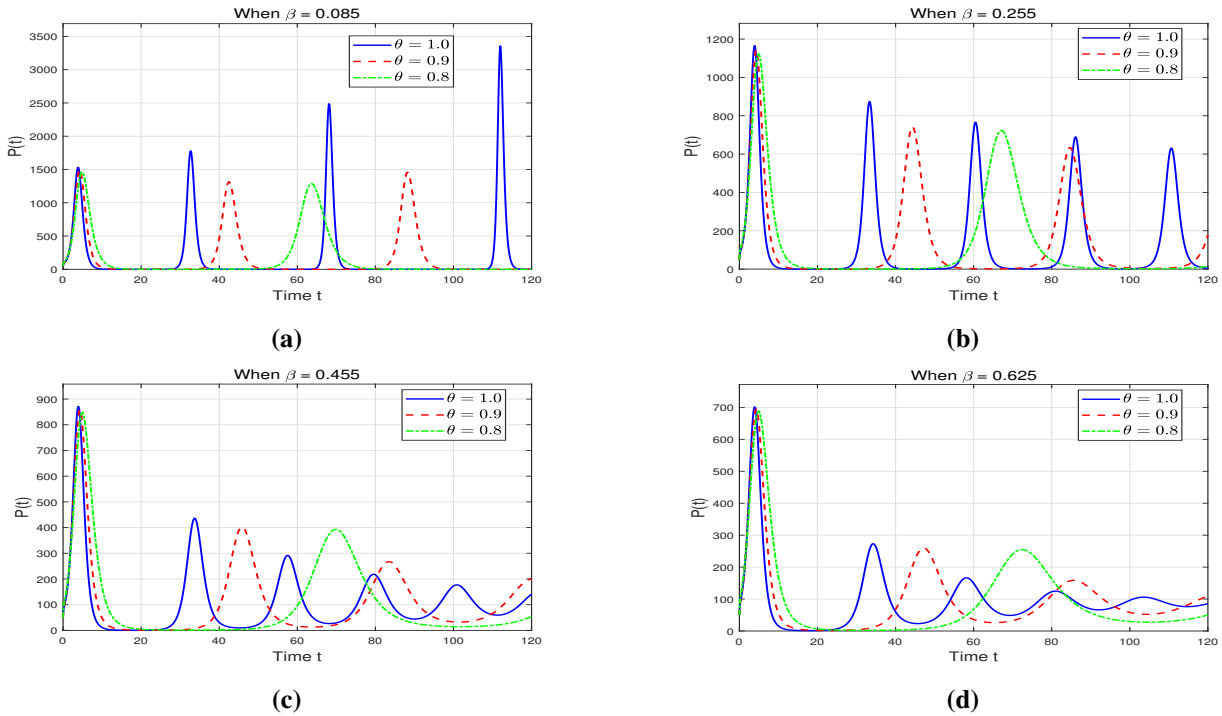

Figure 5. System dynamics under different official rumor-refuting rates, with β set to 0.085, 0.255, 0.455, 0.625 and fractional orders $\theta = 1, 0.9, 0.8$, where panels (a)–(d) show the convergence of $P(t)$ for these parameter sets, respectively.

A quantitative analysis based on Figure 5(a)–(d) identified a significant negative correlation between the official rumor-refuting rate and the size of the rumor-propagator population. The results verified

that official rumor-refuting information can effectively suppress the diffusion and expansion of rumors. Moreover, prioritizing the release of official clarification messages in the initial stage of rumor spread constitutes a highly marginal benefit strategy for public opinion governance and rumor control.

5.4. The existence of Hopf bifurcation

In this study, the rumor-spreading coefficient α and time delay τ are two core bifurcation indicators. We further analyzed the inherent dynamic principles of Hopf bifurcation triggered by the above two parameters in the rumor propagation model.

In the first part of the numerical analysis, the rumor-spreading rate was selected as the dominant bifurcation variable. With all other model parameters maintained unchanged, the fractional order was fixed at $\theta = 1$ for controlled numerical simulation. In this setting, the fractional-order system can be simplified into a standard integer-order dynamic system. By adjusting the value of the spreading coefficient α within a reasonable range and conducting long-term numerical calculations, the evolutionary trend and steady-state performance of the system state variable $F(t)$ were fully monitored.

The numerical results revealed the dynamic variation law of the studied system. Under fixed-parameter conditions, the system equilibrium maintained local asymptotic stability and the entire model remained stable when $\alpha < 3.3 \times 10^{-5}$. As the spreading coefficient continued to increase to $\alpha > 3.3 \times 10^{-5}$, the original stable equilibrium was destroyed, and periodic fluctuation phenomena emerged in the system variables. Moreover, the standard Hopf bifurcation occurred at the critical threshold $\alpha = 3.3 \times 10^{-5}$, which drove the system to transform from a stable equilibrium to periodic oscillation. The bifurcation evolution characteristics are shown in Figure 6.

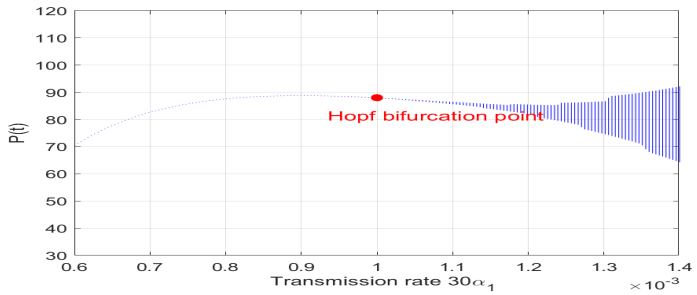

Figure 6. Hopf bifurcation arising from variations in the transmission rate.

Figure 7(a),(b) intuitively reflects how the parameter α affects the steady-state level of rumor-spreading individuals. Figure 7 compares steady-state values under different transmission rates. The steady population of rumor spreaders grows gradually as α increases. This trend tells us that stronger transmission capacity not only triggers oscillation but also raises the baseline number of rumor propagators.

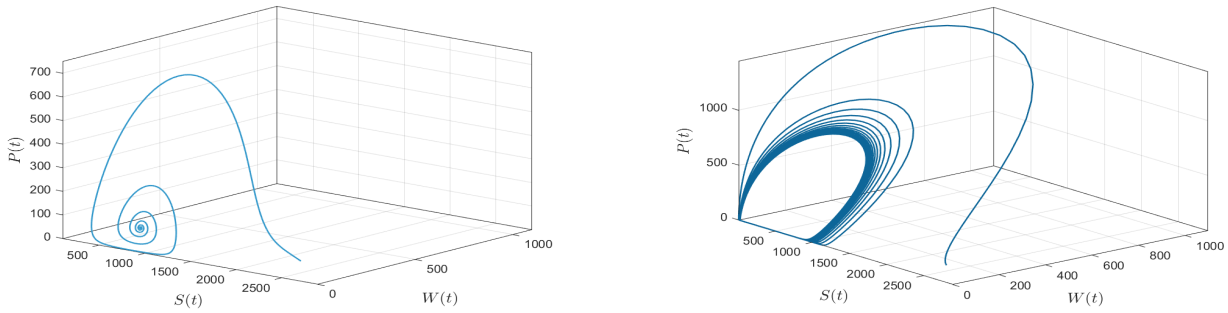

Figure 7. Effects of parameter α on the steady state of rumor propagators, where panels (a) and (b) show that (a) $\alpha < 3.3 \times 10^{-5}$, the rumor-prevailing equilibrium is locally asymptotically stable; (b) $\alpha > 3.3 \times 10^{-5}$, Hopf bifurcation occurs and periodic oscillations emerge.

Remark 3. We note that the direction of Hopf bifurcation and the stability of the bifurcated periodic orbits cannot be judged merely from the characteristic equation. They require higher-order normal-form coefficients obtained by center manifold reduction for fractional delayed systems. Such calculations are algebraically intensive and beyond the scope of the present work. Numerical simulations demonstrate supercritical Hopf bifurcation with stable periodic cycles near $\tau = \tau_0$. Rigorous analytical computation of the normal form will be carried out in our follow-up study.

To explore the effect of time delay on the system stability, we consider τ as the bifurcation parameter and analyze the Hopf bifurcation with the fractional order fixed at $\theta = 0.9$. The number of rumor spreaders $P(t)$ is chosen as the key indicator for characterizing system behavior.

As shown in Figure 8, the system is globally asymptotically stable, with a unique equilibrium for $\tau < 10.47$, where any initial perturbation decays to the steady state. Hopf bifurcation occurs at the critical value $\tau_0 = 10.47$, and the equilibrium loses stability for $\tau > 10.47$.

These results indicate that time delay is a critical factor governing the stability of the system, directly driving the transition from stable to unstable states. Practically, this reveals how the delay from rumor emergence to dissemination influences public opinion dynamics: Small delays allow controllable propagation at a stable level, whereas delays exceeding the threshold break system stability, posing challenges to rumor control and governance.

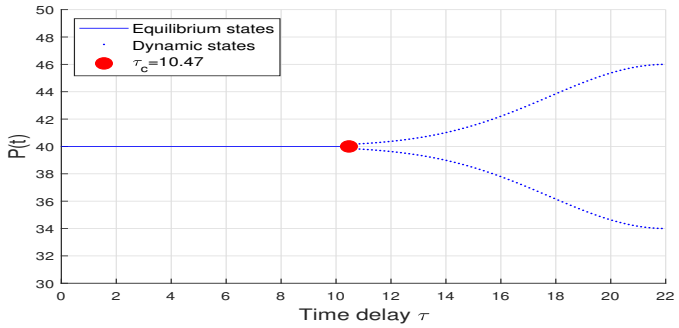

Figure 8. Time delay-induced Hopf bifurcation diagram.

6. Conclusions

This study established a fractional-order SWFPR rumor propagation model that incorporates the fear effect, official rumor refutation mechanism, time delay effect, and fractional-order memory characteristics. The entire population was divided into five subgroups to describe the multistage dynamic evolution of rumor spreading accurately. Using eigenvalue analysis, the Routh–Hurwitz criterion, and Hopf bifurcation theory, the existence and locally asymptotic stability conditions of both rumor-free and rumor-endemic equilibria were systematically derived. Meanwhile, the critical time delay τ_0 that induces Hopf bifurcation was determined, and the system remained stable when $\tau \in [0, \tau_0)$ and became unstable with bifurcation behavior when $\tau > \tau_0$, where the nondegeneracy of the bifurcation was guaranteed by strict verification.

The numerical simulations presented in Figures 2–7 further illustrate the theoretical results derived above. From these plots, we observe that a longer refutation delay tends to trigger periodic rumor outbreaks. The fear effect can suppress the peak density of rumor spreaders, while the fractional order adjusts the strength of memory effects of historical rumor information. Such observations highlight that timely official refutation and reasonable guidance of public fear sentiment are critical for rumor control. Moreover, numerical simulations were conducted to quantify the regulatory effects of key parameters. A smaller fractional order enhances the memory effect and suppresses fluctuations in rumor propagation. A higher fear factor effectively reduces the scale of rumor spread and shortens the attenuation period. Increasing the official rumor refutation rate significantly reduces the density of rumor spreaders and blocks rumor diffusion. An increased rumor transmission rate can trigger oscillations during rumor propagation and further induce system bifurcation. In addition, the increase in the time delay acts as a crucial exogenous driving factor for system instability and bifurcation evolution.

The adopted numerical scheme for fractional delayed differential equations can accurately capture the memory property induced by the fractional order and properly handle the time-delay term. Compared with traditional integer-order numerical algorithms, it is suitable for simulating the long-term dynamical behavior of the SWFPR system and yields reliable bifurcation results.

In future studies, the proposed model will be extended to complex heterogeneous networks with stochastic disturbances, in which the well-mixed mixing assumption is replaced by a topology-dependent contact structure. In that setting, edge-level interventions such as collective influence and edge immunization [25, 26] provide a natural structural complement to the refutation and immunity mechanisms studied here: the homogeneous parameters β and η would become topology-dependent quantities, and the delay threshold τ_0 would be re-derived on the network. We stress, however, that percolation-based containment results and the compartmental stability thresholds derived in this paper are different objects, and the two should be combined rather than directly compared.

In addition, this work concentrates on dynamical behaviors of the uncontrolled SWFPR rumor-propagation system. For practical public-opinion governance, it is worthwhile to further investigate optimal intervention strategies via fractional-order optimal-control theory. Recent 2026 state-of-the-art reinforcement-learning approaches originally developed for malware and epidemic propagation defence provide promising alternative model-free tools for rumor suppression [27]. Standard proximal policy optimization (PPO) exhibits stable policy-update characteristics for

continuous control tasks. Improved variant DC-PPO achieves stronger generalization performance under varying system parameters, while sparse-attention multi-agent reinforcement-learning frameworks mitigate redundant information interactions among agents and are well-suited for large-scale networked spreading scenarios [28].

When adapting these algorithms to our SWFPR rumor-propagation model, several non-trivial challenges remain: (i) Fractional-order memory effects introduce history-dependent state evolution, which violates standard Markov-decision-process assumptions widely adopted in conventional reinforcement-learning implementations. (ii) Time-delay terms further increase state-space complexity and may degrade training convergence. (iii) Real-world rumor intervention requires balancing multiple conflicting objectives: minimizing rumor spread scale while keeping social intervention costs within acceptable bounds.

Therefore, formulating the fractional-order optimal-control problem for SWFPR and developing tailored DC-PPO or sparse-attention multi-agent reinforcement-learning intervention policies constitute important directions for our subsequent study.

Author contributions

Jiaqi Wang: Conceptualization, data curation, formal analysis, investigation, methodology, software, and writing-original draft. Ahmadjan Muhammadhaji: Funding acquisition, project administration, resources, supervision, validation, visualization, and writing-review and editing.

Use of AI tools declaration

The authors declare that they have not used Artificial Intelligence (AI) tools in the creation of this article.

Acknowledgments

This research is supported by the Natural Science Foundation of Xinjiang Uygur Autonomous Region, China (grant No. 2025D01C41), and the Open Project of Xinjiang Key Laboratory of Applied Mathematics (grant No. 2023D04045).

Conflict of interest

The authors declare that there is no conflict of interest.

References

1. D. Daley, D. Kendall, Epidemics and rumours, *Nature*, **204** (1964), 1118. https://doi.org/10.1038/2041118a0
2. D. Daley, D. Kendall, Stochastic rumours, *IMA J. Appl. Math.*, **1** (1965), 42–55. https://doi.org/10.1093/imamat/1.1.42

3. D. Maki, M. Thomson, *Mathematical Models and Applications*, Englewood Cliffs: Prentice-Hall, 1973.
4. H. Wang, L. Deng, F. Xie, H. Xu, J. Han, A new rumor propagation model on SNS structure, in *2012 IEEE International Conference on Granular Computing*, 2012, 499–503. https://doi.org/10.1109/GrC.2012.6468621
5. L. Zhu, X. Zhou, Y. Li, Global dynamics analysis and control of a rumor spreading model in online social networks, *Physica A*, **526** (2019), 120903. https://doi.org/10.1016/j.physa.2019.04.139
6. G. Chen, ILSCR rumor spreading model to discuss the control of rumor spreading in emergency, *Physica A*, **522** (2019), 88–97. https://doi.org/10.1016/j.physa.2018.11.068
7. X. L. Sun, Y. G. Wang, Y. Chai, Y. Liu, Dynamic analysis and control strategies of the SEIHR rumor diffusion model in online social networks, *Appl. Math. Modell.*, **134** (2024), 611–634. https://doi.org/10.1016/j.apm.2024.06.005
8. R. R. Yin, A. Muhammadhaji, Dynamic analysis of rumor propagation model with distributed delay and saturation cure rate in multilingual environment, *Chaos, Solitons Fractals*, **200** (2025), 117055. https://doi.org/10.1016/j.chaos.2025.117055
9. P. Li, R. Gao, C. Xu, Y. Li, A. Akgul, D. Baleanu, Dynamics exploration for a fractional-order delayed zooplankton-phytoplankton system, *Chaos, Solitons Fractals*, **166** (2023), 112975. https://doi.org/10.1016/j.chaos.2022.112975
10. A. De Santis, E. Farsimadan, L. Moradi, F. Palmieri, Generalized defensive modeling of fake news propagation in social networks using fractional differential equations, *IEEE Trans. Comput. Social Syst.*, **12** (2025), 622–634. https://doi.org/10.1109/TCSS.2024.3492097
11. Y. H. Niu, A. Muhammadhaji, Dynamics of a fractional-order IDSR rumor propagation model with time delays, *Fractal Fract.*, **9** (2025), 242. https://doi.org/10.3390/fractalfract9040242
12. M. Cinelli, W. Quattrociocchi, A. Galeazzi, C. M. Valensise, E. Brugnoli, A. L. Schmidt, et al., The COVID-19 social media infodemic, *Sci. Rep.*, **10** (2020), 16598. https://doi.org/10.1038/s41598-020-73510-5
13. R. H. Knapp, A psychology of rumor, *Public Opin. Q.*, **8** (1944), 22–37. https://doi.org/10.1086/265665
14. N. Stieglitz, L. D. Xuan, Emotions and information diffusion in social media: Empirical analysis of the 2011 Japanese earthquake, *J. Manage. Inf. Syst.*, **30** (2013), 251–278.
15. S. Pfattheicher, Anxiety and the acceptance of vaccine side-effect rumors during the COVID-19 pandemic, *J. Appl. Social Psychol.*, **51** (2021), 389–402.
16. Y. Zhao, Z. Li, W. Wang, Rumor spreading model with time delay and heterogeneous refutation in complex networks, *Physica A*, **556** (2020), 124834.
17. Y. Y. Cheng, L. A. Huo, L. J. Zhao, Dynamical behaviors and control measures of rumor-spreading model in consideration of the infected media and time delay, *Inf. Sci.*, **564** (2021), 237–253. https://doi.org/10.1016/j.ins.2021.02.047
18. L. H. Zhu, G. Guan, Dynamical analysis of a rumor spreading model with self-discrimination and time delay in complex networks, *Physica A*, **533** (2019), 121953. https://doi.org/10.1016/j.physa.2019.121953

19. P. A. Naik, M. Yavuz, S. Qureshi, M. Naik, K. M. Owolabi, A. Soomro, A. H. Ganie, Memory impacts in hepatitis C: A global analysis of a fractional-order model with an effective treatment, *Comput. Methods Programs Biomed.*, **254** (2024), 108306. https://doi.org/10.1016/j.cmpb.2024.108306

20. V. Madhusudanan, P. A. Naik, B. S. N. Murthy, L. Guerrini, M. N. Srinivas, L. Chada, Modeling tuberculosis transmission with kernel functions: Effects of vaccination and time delay, *Eur. Phys. J. Plus*, **141** (2026), 76. https://doi.org/10.1140/epjp/s13360-026-07309-0

21. A. Muhammadhaji, Y. H. Niu, Stability and hopf bifurcation of a delayed fractional-order ISR rumor propagation model with saturation incidence, *Fractal Fract.*, **10** (2026), 708. https://doi.org/10.3390/fractalfract10100708

22. T. Zhou, A. Muhammadhaji, Dynamics in a fractional-order competitive-competitive-cooperative system with Beddington-Deangelis functional responses and delay, *Fractal Fract.*, **10** (2026), 176. https://doi.org/10.3390/fractalfract10030176

23. M. Mandal, S. Jana, S. K. Nandi, T. K. Kar, Modelling and control of a fractional-order epidemic model with fear effect, *Energy Ecol. Environ.*, **5** (2020), 421–432. https://doi.org/10.1007/s40974-020-00192-0

24. J. Y. Zhang, Y. K. Xue, G. Q. Hu, Analysis of fractional order SVEIR infectious disease model with fear effect and secondary vaccination, *Nonlinear Dyn.*, **113** (2025), 34047–34065. https://doi.org/10.1007/s11071-025-11752-6

25. X. Zhang, J. C. Li, Y. L. Ma, M. H. Wang, Dynamic modelling and analysis of online rumour propagation considering dual debunking mechanisms and time delay effects, *Humanit. Social Sci. Commun.*, **13** (2026), 905. https://doi.org/10.1057/s41599-026-07243-7

26. Y. Liu, G. Liang, X. Wang, P. Zhu, Z. Wang, Diffusion containment in complex networks through collective influence of connections, *IEEE Trans. Inf. Forensics Secur.*, **19** (2024), 1510–1524. https://doi.org/10.1109/TIFS.2023.3338423

27. G. Liu, J. Zhu, Q. Li, C. Zhang, W. Jiang, X. Zhong, et al., Networked spatiotemporal optimal control and DC-PPO reinforcement learning for combating malware spread in IoUT , *IEEE Trans. Network Sci. Eng.*, **13** (2026), 10252–10269. https://doi.org/10.1109/TNSE.2026.3692250

28. G. Liu, C. Wang, T. Tan, D. Shen, G. Fortino, G. Franze, et al., A fractional-order game-theoretic model with sparse attention multi-agent reinforcement learning for malware defense in IoV, *IEEE Trans. Autom. Sci. Eng.*, 2025, 3950–3966. https://doi.org/10.1109/TASE.2025.3641288



AIMS Press

© 2026 the Author(s), licensee AIMS Press. This is an open access article distributed under the terms of the Creative Commons Attribution License (https://creativecommons.org/licenses/by/4.0)